Supporting Information

Madeira da Silva and Beverley 10.1073/pnas.1004599107

SI Text

Gene Replacement Constructs. In all studies, we sought to replace TOR ORFs with ones encoding independent selectable markers. Deletion cassettes were constructed by the fusion-PCR technique (1). Table S2 shows the sequences of all primers used.

Generation of *L. major tor3*$^{-}$. First, the ORFs of the selectable markers puromycin (*PAC*, 600 bp) and hygromycin (*HYG*, 1026 bp) were amplified with primers SMB2561/2562 and SMB2557/2558, respectively, each bearing generic linker sequences. Then, using *L. major* FV1 genomic DNA as template, the *TOR3* 5′and 3′ flanking sequences (867 bp and 813 bp) were amplified by PCR with primers SMB2647/2648 (added BamHI site) and SMB2649/2650 (added NdeI site for PAC cassette) or SMB2649/2901 (added SpeI for HYG cassette). A second round of PCR was conducted using the three fragments amplified in the first round PCR as templates, now using the external primers SMB2647/2650 (PAC) or SMB2647/2901(HYG). The full-length constructs were then cloned in pGEM-T Easy, yielding *TOR3* replacement constructs (B6006 and B6027, respectively). The replacement cassettes were released from these plasmids by double digestion with BamHI/NdeI or BamHI/SpeI, respectively, and the DNA fragments were dephosphorylated with calf intestinal phosphatase previously to the transfections.

To generate the *tor3*$^{-}$ mutant parasites, *L. major* FV1 was transfected with the *TOR3::*Δ*HYG* fragment by electroporation (2). Cells were plated semisolid M199 media containing 50 μg/mL hygromycin B to recover clonal lines. Two lines showing correct integration of the replacement cassette by PCR tests were inoculated at high levels (10^7) into Balb/C mice; both developed lesions comparable to those in WT parasites, and were recovered by aspiration of the infected foot after 2 wk. Clone *TOR3*/Δ*TOR3*::*HYG* H4 was chosen for targeting the remaining *TOR3* allele with the *TOR3::*Δ*PAC* replacement cassette, and transfections and plating on media containing 50 μg/mL hygromycin B and 30 μg/mL puromycin were performed as in the prior step. PCR analysis identified five clonal lines showing correct integration of the second replacement cassette and lack of *TOR3* ORF by PCR. Three such Δ*TOR3*::*HYG*/Δ*TOR3*::*PAC* lines were inoculated as before in the footpad of Balb/C mice, and none resulted in lesion development, even after 1 y. We chose clones Δ*TOR3*::*HYG*/Δ*TOR3*::*PAC* H4P1 and H4P3 for the characterization of the mutant phenotype; both were similar, and only the results of clone H4P3 (referred to as *tor3*$^{-}$ hereafter) are shown. A similar set of studies were performed using first the *TOR3*::Δ*PAC* and then the *TOR3*::Δ*HYG* construct, again yielding null mutant parasites that failed to show lesion pathology after inoculations.

A construct for restoring *TOR3* expression was made as follows: the full-length TOR3 ORF (7,787-bp) was amplified by two-step PCR with Phusion Polymerase (Finnzymes) using *L. major* FV1 DNA as template and primers SMB2908/2909, which added BclI sites at the 5′ and 3′ ends of the ORF and a Myc-tag at the N terminus of *TOR3*. The full-length amplified fragment was inserted into pGEM-T easy, yielding pGEM-*MycTOR3* (B6325), and transformed into a *dam*$^{-}$ strain of *E. coli*. The *TOR3* insert was completely sequenced with plasmid primers (SMB2495 and SMB2496) and 12 internal primers (SMB2843–SMB2854). The *MycTOR3* sequence was released by BclI digestion and then inserted into the BglII site of pXNG4SAT4 (3), yielding pXNG4SAT-MycTOR3 (B6037); the correct orientation was confirmed by sequencing with primers SMB1297 and SMB1298. This plasmid was then introduced into the *tor3*$^{-}$ clonal lines Δ*TOR3*::*HYG*/Δ*TOR3*::*PAC* H4P1 and H4P3. Tests of 10 clonal lines inoculated at high levels (10^7) into Balb/C mice all showed pathology after 2 wk. Clones H4P1AB3 and H4P3AB2 were chosen for further studies, hereafter called *tor3*$^{-}$/+ *TOR3* (results with H4P3AB2 are shown). pXNG4SAT4-MycTOR3 was also introduced into WT *L. major* FV1.

Attempts to Knock Out *L. major TOR1* and *TOR2*. Replacement constructs for *TOR1* and *TOR2* were made in a manner analogous to that described for *TOR3* above (details available on request). We attempted to generate null mutant cell lines for each of the TOR kinases genes in *L. major*; however, we could not obtain knockouts for *TOR1* and *TOR2* (Fig. S3 *A* and *B*).

The replacement of the first allele of *TOR1* was easily obtained with either of the two replacement cassettes containing resistance to puromycin (*PAC*) or nourseothricin (*SAT*) as verified by PCR for five and 12 clones, respectively (Fig. S3*A*). This confirmed the functionality of both cassettes. However, we did not obtain any colonies after transfecting the heterozygous *TOR1*$^{+/-}$ parasites to replace the second allele of this gene in five independent transfections with the *PAC* cassette and two transfections with *SAT* cassette. Positive control transfections with pXGPAC or pXGSAT resulted in several hundred colonies for each transfection.

Similarly, for *TOR2* heterozygotes with either *BSD* or *HYG* markers were readily obtained following transfection (Fig. S3*B*). Unlike the results above with TOR1, transfections of *BSD*/+ or *HYG*/+ heterozygotes with *HYG* or *BSD* targeting constructs respectively did yield progeny. However, PCR tests of all such transfectants retained *TOR2*, and analysis of 21 further confirmed the presence and proper integration of both resistance markers into the TOR2 locus (Fig. S3*B*). This phenomenon is often seen when targeting essential genes in *Leishmania*, and arises through the generation of extra copies of the target locus by polyploidy or aneuploidy, yielding cells bearing both the correct planned replacements but retaining the target gene (4). Analysis of DNA content of 10 doubly-resistant transfectants showed that they had normal DNA contents, suggesting that the extra copy of the *TOR2* locus arose by aneuploidy.

Western Blotting. Promastigote lysates were prepared by suspending parasites in 1× Laemmli loading buffer and immediately boiling for 5 min. Samples (3×10^6 cell equivalents/lane) were subjected to SDS/PAGE and electrotransferred to nitrocellulose membranes (Hybond-ECL, Amersham Biosciences). Membranes were blocked with 5% nonfat dry milk in TBST (20 mM Tris·base, pH 7.6, 140 mM sodium chloride, 0.05% Tween 20) for 1 h at room temperature. Protein loading was assessed with a rabbit anti–*L. major* histone H2A polyclonal antibody at 1:100,000 dilution. Polyclonal rabbit antibody anti-GFP (Abcam) was used at 1:2,000 dilution, anti-HASPB (5) at 1:5,000 dilution, and monoclonal 9E10 anti-Myc antibody (BD Biosciences) at 1:500 dilution. Goat antirabbit IgG HRP-conjugated secondary antibody (Jackson ImmunoResearch) was used at 1:10,000, and antimouse IgG HRP-conjugated secondary antibody (Amersham Biosciences) at 1:5,000. ECL reactions were revealed with a PerkinElmer Life Sciences chemiluminescence kit.

Transmission EM. Parasites were fixed in 2% paraformaldehyde/2.5% glutaraldehyde (Polysciences) in 100 mM phosphate buffer, pH 7.2, for 1 h at room temperature. Samples were washed in phosphate buffer and postfixed in 1% osmium tetroxide (Polysciences) for 1 h, and then rinsed extensively in H_20 before en

bloc staining with 1% aqueous uranyl acetate (Ted Pella.) for 1 h. Following several rinses in H_20, samples were dehydrated in a graded series of ethanol and embedded in Eponate 12 resin (Ted Pella Inc.). Sections of 90 nm were cut with a Leica Ultracut UCT ultramicrotome (Leica Microsystems), stained with uranyl acetate and lead citrate, and viewed on a JEOL 1200 EX transmission electron microscope (JEOL USA). The area of individual ACs in the cross-sections was measured by Volocity software (Improvision; PerkinElmer), and diameter of the organelles was inferred from the area values assuming their circular shape.

Immunofluorescence Microscopy. Immunofluorescence microscopy to visualize ACs was performed with rabbit polyclonal anti-TbVP1 antibody, kindly provided by Roberto Docampo (6). Promastigotes were washed twice with 1× DPBS (Dulbecco's phosphate buffered saline; Cellgro, Mediatech) and fixed with 4% paraformaldehyde for 30 min. Cells were then permeabilized with 100% cold methanol for 10 min on ice and rehydrated in 1× DBPS for 10 min at room temperature. Blocking was performed for 1 h with 10% normal goat serum, 3% BSA, 50 mM NH_4Cl in 1xDPBS. Next, cells were incubated with anti-TbVP1 (1:300) for 1 h, washed, and finally incubated with 1:1,000 diluted antirabbit IgG Alexa 595–conjugated antibody (Invitrogen). Coverslips were mounted with ProLong Gold antifade reagent (Invitrogen). Visualization of fluorescence was performed in a Zeiss LSM 510 Meta confocal microscope (Carl Zeiss).

Polyphosphate Detection with DAPI by Fluorescence Microscopy. Inorganic polyphosphate content in the ACs was evaluated by staining the cells with DAPI as described (7). Promastigotes (2×10^6 cells per coverslip) were washed twice with 1× DPBS, fixed with 4% paraformaldehyde for 30 min, and then incubated with 50 μg/mL DAPI for 15 min at room temperature. Coverslips were directly mounted in slides for immediate visualization in a fluorescence microscope (Olympus AX70) using UV excitation (350 nm) and a long-pass emission filter >460 nm. Images were captured by a QImaging RETIGA 200R FAST color camera with an RGB adaptor (Chroma Technology), at the same exposure time and nonsaturating conditions.

1. Szewczyk E, et al. (2006) Fusion PCR and gene targeting in Aspergillus nidulans. *Nat Protoc* 1:3111–3120.
2. Robinson KA, Beverley SM (2003) Improvements in transfection efficiency and tests of RNA interference (RNAi) approaches in the protozoan parasite Leishmania. *Mol Biochem Parasitol* 128:217–228.
3. Murta SM, Vickers TJ, Scott DA, Beverley SM (2009) Methylene tetrahydrofolate dehydrogenase/cyclohydrolase and the synthesis of 10-CHO-THF are essential in Leishmania major. *Mol Microbiol* 7:1386–1401.
4. Cruz AK, Titus R, Beverley SM (1993) Plasticity in chromosome number and testing of essential genes in Leishmania by targeting. *Proc Natl Acad Sci USA* 90:1599–1603.
5. McKean PG, Denny PW, Knuepfer E, Keen JK, Smith DF (2001) Phenotypic changes associated with deletion and overexpression of a stage-regulated gene family in Leishmania. *Cell Microbiol* 3:511–523.
6. Lemercier G, et al. (2002) A vacuolar-type H+-pyrophosphatase governs maintenance of functional acidocalcisomes and growth of the insect and mammalian forms of Trypanosoma brucei. *J Biol Chem* 277:37369–37376.
7. Fang J, et al. (2007) Overexpression of a Zn2+-sensitive soluble exopolyphosphatase from Trypanosoma cruzi depletes polyphosphate and affects osmoregulation. *J Biol Chem* 282:32501–32510.
8. Thompson JD, Higgins DG, Gibson TJ (1994) CLUSTAL W: Improving the sensitivity of progressive multiple sequence alignment through sequence weighting, position-specific gap penalties and weight matrix choice. *Nucleic Acids Res* 22:4673–4680.
9. Kumar S, Tamura K, Nei M (2004) MEGA3: Integrated software for Molecular Evolutionary Genetics Analysis and sequence alignment. *Brief Bioinform* 5:150–163.
10. Kelley LA, Sternberg MJ (2009) Protein structure prediction on the Web: A case study using the Phyre server. *Nat Protoc* 4:363–371.

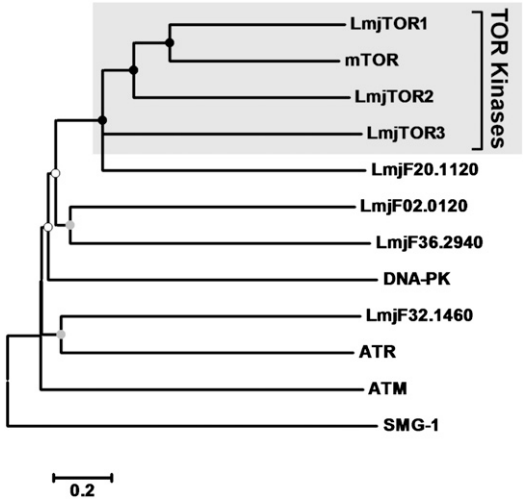

Fig. S1. Phylogenetic tree of *L. major* TOR-related kinases and selected outgroup PIKKs. The phylogenetic tree was constructed using the Mega 3.1 package, starting with a ClustalW alignment of the full-length amino acid sequences (8, 9). The Neighbor-Joining algorithm was then used to calculate the consensus tree shown. Bootstrap confidence limits calculated from 1,000 replicates are shown; values ≥99% are represented by black nodes, values >70% by gray nodes, and values <50% by white nodes.

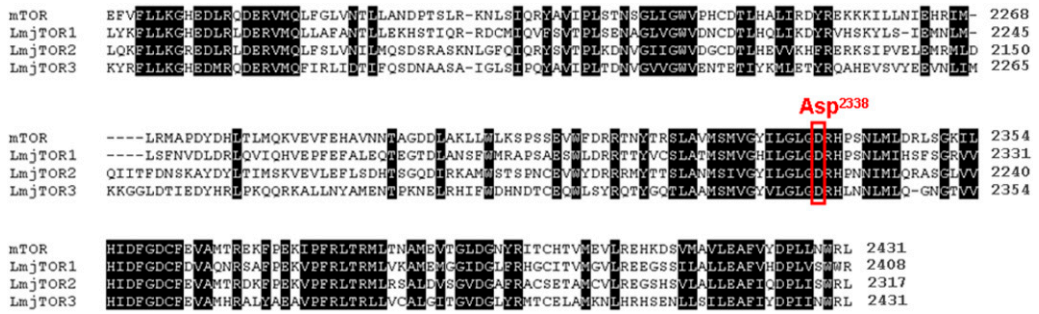

Fig. S2. Multiple alignment of the catalytic PI-kinase domain of TORs comparing the three *L. major* TORs and human mTOR. Black shading corresponds to residues 100% conserved in all sequences. Conservation of a crucial residue for TOR kinase activity in all *L. major* TORs (Asp^{2338} in mTOR) is highlighted.

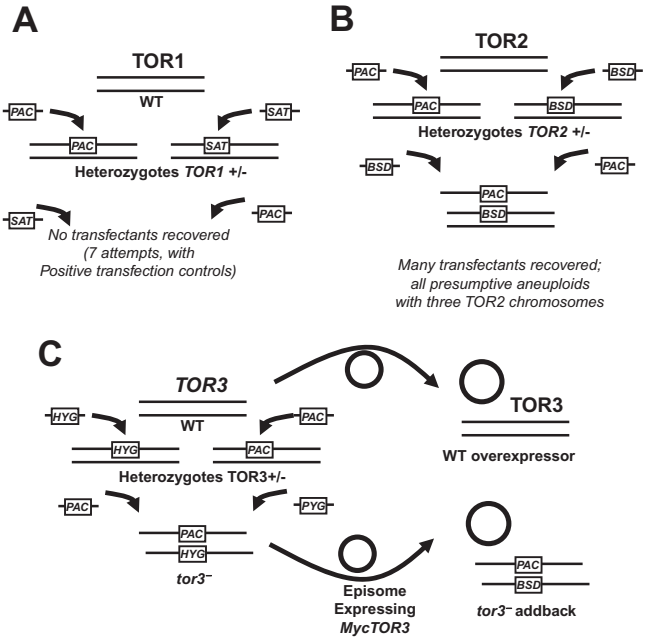

Fig. S3. Schematic diagram of strategies used to generate null mutants of *L. major* TOR kinases. (*A*) *TOR1*. Replacement of the first *TOR1* allele by either *PAC* or *SAT* targeting fragments was readily achieved. However, transfections of either the *SAT* or *PAC* targeting fragments into the lines above respectively yielded no colonies in a total of seven experiments. In every experiment, positive control transfections (pXGPAC or pXGSAT) yielded several hundred colonies. (*B*) TOR2. Replacement of the first *TOR2* allele by either *BSD* or *PAC* targeting fragments was readily achieved. Transfections of either the *PAC* or *BSD* targeting fragments into the lines above, respectively, also yielded many colonies. However, PCR tests of 21 lines showed that all retained three copies of the *TOR2* chromosome, one copy containing the planned *PAC* replacement, one copy containing the planned *BSD* replacement, and one copy bearing TOR2. The DNA content of these was similar to that of WT, suggesting that these lines had likely arisen by aneuploidy, as seen in other tests of essential genes in *Leishmania* (4). (*C*) *TOR3*. Successive replacement of *TOR3* by *HYG* and then *PAC* targeting constructs occurred readily (Fig. S4). Restoration of *TOR3* expression was accomplished by transfection of pXNG4SAT-MycTOR3 as a circular episome; this construct was also introduced in the WT line. *Leishmania* episomal expression vectors typically exist in a copy of ~30, which often results in protein overexpression.

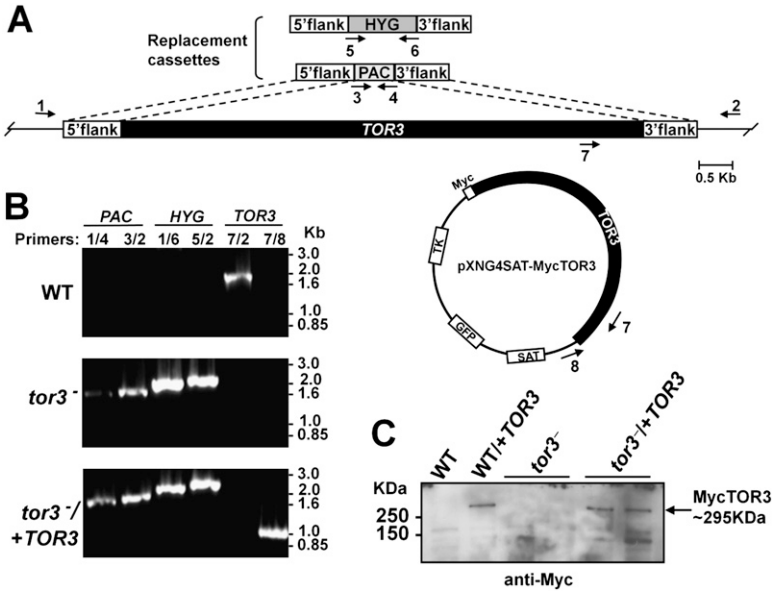

Fig. S4. Generation of *L. major tor3*$^{-}$ null mutant promastigotes. (*A*) Map of the WT TOR3 locus and replacement targeting cassettes used. Drug resistance markers: puromycin (*PAC*) and hygromycin B (*HYG*). Arrows indicate position of primers used to confirm integration of the cassettes in the correct genomic locus. (*B*) PCR analysis of a representative knockout line (*tor3*$^{-}$) and an "addback" line (*tor3*$^{-}$/+*TOR3*). Primers 1 and 4 and primers 3 and 2 confirm the 5′ and 3′ position of the *PAC* replacement; primers 1 and 6 and primers 5 and 2 confirm the 5′ and 3′ position of the *HYG* replacement; primers 7 and 2 confirm the presence or absence of the *TOR3* ORF in its genomic context; and primers 7 and 8 confirm the presence or absence of the *TOR3* ORF in the plasmid context. Primers are as follows: primer 1, SMB2765; 2, SMB2810; 3, SMB2557; 4, SMB2558; 5, SMB2561; 6, SMB2562; 7, SMB2854; 8, SMB1298 (Table S2). (*C*) Western blotting of total lysates of *L. major* promastigotes (5×10^6 cells per lane) with anti-Myc antibody confirms the expression of *MycTOR3* in a representative line of WT/+*TOR3* (lane 2), and two lines of *tor3*$^{-}$/+*TOR3* (lanes 5 and 6). WT (lane 1) and two lines of *tor3*$^{-}$ (lanes 3 and 4) are negative controls. Arrow points to the band of expected size of *MycTOR3*.

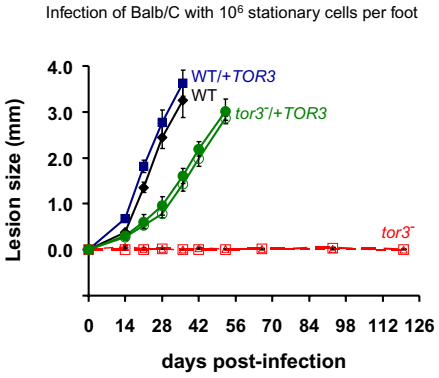

Fig. S5. *L. major tor3*$^{-}$ have attenuated virulence in mice. Balb/C mice were infected with 10^6 stationary cells and lesion progression was measured over time. WT (■), WT/+*MycTOR3* (◆), two clones of *tor3*$^{-}$ (○, Δ) and two clones of *tor3*$^{-}$/+*MycTOR3* (□, ▲). Error bars show SEM of results of four mice used for each group.

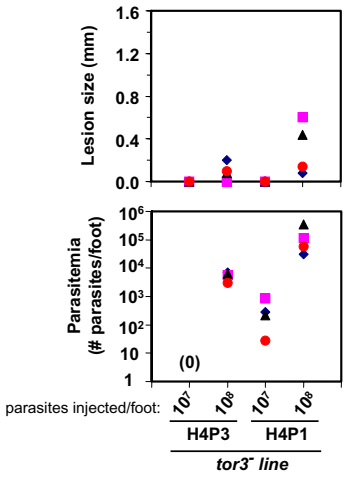

Fig. S6. Mouse infections using large numbers of *L. major tor3*$^{-}$ stationary phase cells. Limiting dilution assay was performed at day 21 postinfection to determine the parasitemia (*Lower*) in Balb/C mice infected with 10^7 or 10^8 stationary cells per foot. We used two clones of *tor3*$^{-}$, H4P1 and H4P3. Lesions were measured at day 21 (*Upper*). We did not recover parasites from mice infected with 10^7 stationary cells for clone H4P3. Symbols represent data for individual mice (one to four within each group).

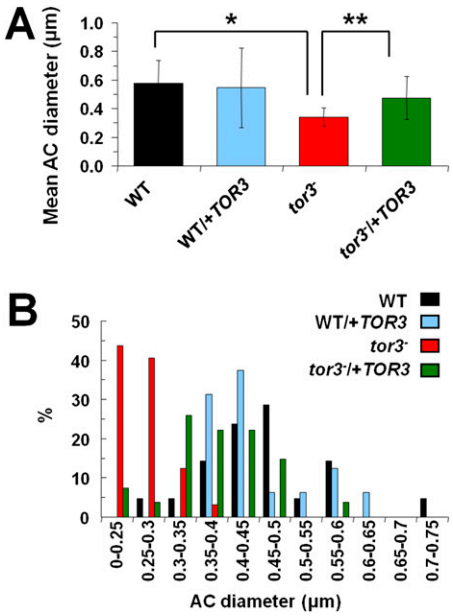

Fig. S7. Quantification of ACs shows that ACs of *tor3*$^{-}$ parasitesare significantly smaller. (*A*) Average diameter and (*B*) distribution of ACs. Late logarithmic phase promastigotes were fixed and subjected to transmission EM. The AC diameter was measured using the Volocity software package (Perkin-Elmer), assuming a circular shape. The number of cells measured was: WT, n = 20 cells (163 ACs); WT/+*TOR3*, n = 16 cells (149 ACs); *tor3*$^{-}$, n = 32 cells (150 ACs); and *tor3*$^{-}$/+*TOR3*, n = 27 cells (202 ACs). Statistical analysis used the Student t test for two samples (*P < 6e-44; **P < 2e-21).

Table S1. Members of the family of PIKK in *L. major*

Gene ID	Presence of FRB domain		Pairwise Blast full-length sequences			Pairwise Blast 1,200 residues of C terminus		
	Pfam score (*E*-value)	Phyre % precision (*E*-value)*	Length of overlap	%ID (% similarity)	*E* -value	Length of overlap	%ID (% similarity)	*E* -value
LmjF36.6320 (LmjTOR1)	180 (6.7e-51)	100% (6.3e-18)	2,049 aa	28% (43%)	0.0	1,143 aa	36% (46%)	e-157
LmjF34.4530 (LmjTOR2)	191 (2.3e-54)	100% (1.6e-18)	2,328 aa	24% (41%)	e-179	1,060 aa	33% (50%)	e-156
LmjF34.3940 (LmjTOR3)	147 (5.3e-41)	100% (6.1e-15)	1,314 aa	26% (44%)	e-125	1,077 aa	27% (46%)	e-116
LmjF20.1120	Not found	Not found	1,354 aa	25% (41%)	8e-95	1,127 aa	26% (43%)	5e-90
LmjF32.1460	Not found	Not found	269 aa	30% (55%)	9e-35	269 aa	30% (55%)	3e-35
LmjF02.0120	Not found	Not found	390 aa	28% (43%)	6e-31	390 aa	28% (43%)	2e-31
LmjF36.2940	Not found	Not found	315 aa	27% (44%)	6e-21	315 aa	27% (44%)	2e-21

BLAST searches using mTOR as query against the database of *L. major* predicted proteins (GeneDB) retrieved seven top hits. Comparisons between each to mTOR were performed by Pairwise Blast (BLAST 2 sequences) for the full-length sequences or only the last 1,200 residues of the C terminus. The presence of the FRB domain, which is unique to TOR kinases, was confirmed by searches in Pfam domain database. Finally, regions corresponding to the Pfam-identified FRB domains were used as queries to the structure prediction server Phyre (10).

*Estimated precision score (%) and E-value refer to modeling the predicted *L. major* FRBs to the template structure of mTOR FRB (SCOP code: c2npuA) in the Phyre fold library).

Table S2. Sequences of oligonucleotide primers used

Primer no.	Sequence (5′–3′)
Primers used to make knockout constructs	
SMB2647	GGATCCGGCTCTGGACTCAAGTTTGC
SMB2648	**CGTCAGCCCGCACCGTTACC**AGCGACTCTGCCATTGTGC
SMB2649	**GCACCTTACGTGGGATCTCG**AGGATCGTCAAGCCCAGC
SMB2650	CATATGGGAGAAGGGCCTCGACATAC
SMB2901	ACTAGTGGAGAAGGGCCTCGACATAC
SMB2557	**GGTAACGGTGCGGGCTGACG**CCACCATGACCGAGTACAAGCCC
SMB2558	**CGAGATCCCACGTAAGGTGC**TCAGGCACCGGGCTTGCG
SMB2561	**GGTAACGGTGCGGGCTGACG**CCACCATGAAAAGCCTGAACTC
SMB2562	**CGAGATCCCACGTAAGGTGC**CTATTCCTTTGCCCTCG
Primers used to make Myc-tagged TORc addback	
SMB2908	TGATCAATGgaacaaaaactcatctcagaagaggatctgGCAGAGTCGCTGGCCCCA
SMB2909	TGATCACTACCAGAAAGGTGCCCAGCCG
SMB2843	Ctggtgacactgaaggatgc
SMB2844	Agcgatctcgaggtgaagtc
SMB2845	Atatcacccgacggttgtg
SMB2846	Agatggaggaggaggaggtg
SMB2847	Tgcagtaatgcacgagaagg
SMB2848	Catgatcgacttccgctttc
SMB2849	Cggaacgaggtgttattgtg
SMB2850	Gtgctgcggtgtgagcag
SMB2851	Ctcgaggtcctatgcgagtg
SMB2852	Cctgaccgacttgctcattc
SMB2853	Tatacgtgatgccgtccaag
SMB2854	Ccatctcaacaacctgatgc
SMB2495	GTTTTCCCAGTCACGAC
SMB2496	CAGGAAACAGCTATGAC
SMB1297	TTTCACTTGCTCTCCCCT
SMB1298	AGCCGGAAGTGCTGGCAT
Primers used to confirm integration of knockout cassettes	
SMB2765	AGTGCTCTGAACGGCATCTG
SMB2810	GTGTTGCTGGTCTCATGTGC

Underlined data indicate restriction sites. Boldface data indicate linker sequence for fusion PCR. Small capital letters indicate Myc-tag.